Research Article

Rapid Communications in Mass Spectrometry

Received: 24 July 2012 Revised: 16 August 2012 Accepted: 22 August 2012 Published online in Wiley Online Library

Rapid Commun. Mass Spectrom. **2012**, *26*, 2502–2508
(wileyonlinelibrary.com) DOI: 10.1002/rcm.6374

Tandem mass spectrometric analysis and density functional theory calculations on the fragmentation behavior of two tetradecanoylingenol regioisomers from *Euphorbia wallichii*

Bing Xia[1†], Kaijie Xu[1†], Xin Liu[2], Yunfeng Chai[3], Cuirong Sun[3], Yucheng Gu[4], Lisheng Ding[1] and Yan Zhou[1*]

[1]Key Laboratory of Mountain Ecological Restoration and Bioresource Utilization, Chengdu Institute of Biology, Chinese Academy of Sciences, Chengdu 610041, P.R. China
[2]Beijing Entry-Exit Inspection and Quarantine Bureau, Beijing 100026, P.R. China
[3]Department of Chemistry, Zhejiang University, Hangzhou 310027, P.R. China
[4]Syngenta Jealott's Hill International Research Centre, Bracknell, Berkshire RG42 6EY, UK

RATIONALE: Two structurally similar bioactive regioisomers, 3-*O*-tetradecanoylingenol and 20-*O*-tetradecanoylingenol, from *Euphorbia wallichii* presented quite different fragmentation behaviors. Revealing the related fragmentation pathways may improve the efficiency of characterization and identification of such type of compounds.
METHODS: The two regioisomers were subjected to collision-induced dissociation (CID) on Finnigan LCQ^{DECA} and LTQ Orbitrap XL instruments. Based on the CID results, the possible fragmentation pathways were proposed and investigated with density functional theory (DFT) calculations.
RESULTS: Elimination of $C_{14}H_{28}O_2$ (tetradecanoic acid) for 3-*O*-tetradecanoylingenol and the sequential losses of C_4H_8 (butylene) for 20-*O*-tetradecanoylingenol were observed in ESI-MS/MS, witnessed also by HR-ESI-MS/MS. The fragmentation pathways were proposed and verified by calculating the activation energy of their transition states by DFT calculations.
CONCLUSIONS: Based on the observations, fragmentation pathways for the two regioisomers were proposed and verified by calculating the energy of the reactants, products and the corresponding transition states using DFT. This report should have value in rapid identification of the derivatives of ingenol and other regioisomers in natural products.

Tandem mass spectrometry (MS/MS) has been increasingly applied in the field of natural product chemistry for characterization and identification of active components from the complex matrices of herbal medicines extracts so as to avoid tedious separation.[1–4] For that purpose, fragmentation mechanisms and empirical formula calculation are very important for structural elucidation in combination with other available analytical methods. However, it is still a difficult task to differentiate the isomers by MS/MS.

Fragmentation of a molecular ion in MS/MS is complex which depends on many conditions such as the three-dimensional structure of the ion, the internal energy obtained during collision and the stability of the product ions. DFT calculations have become a very powerful tool to aid the interpretation of experimentally obtained MS/MS spectra. Much research in mass spectrometry uses DFT calculations to predict the energies of the reactants, transition states, intermediates and products to find the most favorable reaction pathways involved in the fragmentation processes.[5–8] In a word, the computer-aided elucidation of MS/MS spectra makes the proposed fragmentation pathways more rational.

Ingenane-type diterpenoids are the main components of *Euphorbia wallichii* Hook. f. Fl.*E*.,[9–11] and many of them were demonstrated to have dramatic biological activities. For example, ingenols were found to possess antineoplastic and cytotoxic activities, tumor promotion, skin irritancy, molluscicide, and antiviral activities,[12–21] and some of the ingenane derivatives were proved to have anticancer activities.[22] Due to the slight difference in the complicated structures of these ingenane derivatives, it has always been a challenge to identify these analogues.

We here report the ion trap electrospray ionization (ESI)-MS/MS analyses of two regioisomers, 3-*O*-tetradecanoylingenol (**M1**) and 20-*O*-tetradecanoylingenol (**M2**) (Fig. 1), representing the major components found in the total extracts of *E. wallichii*. The ion trap mass analyzer has allowed us to obtain spectra up to MS^4 that are rich in information and have shown typical losses. The implementation of the LTQ Orbitrap MS instrument for the measurement of accurate molecular masses, and the

* *Correspondence to:* Y. Zhou, Key Laboratory of Mountain Ecological Restoration and Bioresource Utilization, Chengdu Institute of Biology, Chinese Academy of Sciences, Chengdu 610041, P.R. China.
E-mail: zhouyan@cib.ac.cn

† These authors contributed equally to this study.

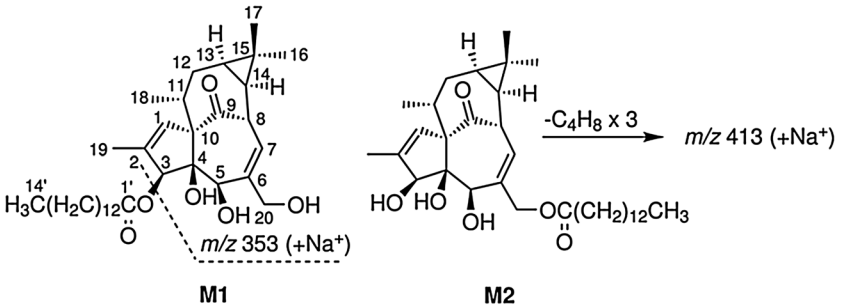

Figure 1. Structures and the key fragmentations of **M1** and **M2** from *Euphorbia wallichii*.

identity confirmation of the fragment ions, were demonstrated an effective analytical method. Both sets of data are combined and used to construct fragmentation pathways of the two ingenol regioisomers. As a result, the diagnostic fragment patterns of the two regioisomers were summarized, and the proposed fragment pathways were verified by calculating the activation energies of their transition states using density functional theory (DFT). ESI-MS^n in combination with DFT calculations has proved to be an effective tool in the structural elucidation of isomers of natural product compounds.

EXPERIMENTAL

Chemicals and reagents

M1 and **M2** were isolated from the roots of *E. wallichii* in our laboratory and their structures were elucidated by MS, 1D and 2D NMR evidence. The purity of each compound was determined to be higher than 98% by high-performance liquid chromatography (HPLC) detection. The samples were dissolved in pure methanol (HPLC grade, Aldrich Chemicals) at a concentration of 10 μM and were ready for analysis by ESI-MS/MS within 15 min.

Mass spectrometry

Mass and tandem mass spectra were obtained on a Finnigan LCQ^{DECA} (San Jose, CA, USA) ion-trap mass spectrometer equipped with an ESI source. The instrument was operated in the positive ion mode with the experimental parameters as follows: nebulizer sheath gas, N_2 (20 units); capillary temperature 250 °C; spray voltage 4.5 kV; capillary voltage 15 V. The MS/MS experiments were carried out by setting the normalized collision energy to 25% (for **M1**) and 40% (for **M2**), and a mass range of *m/z* 50–2000 was scanned. The precursor ion isolation window was set at 2 Da to maximize signal/noise in MS/MS. Samples were continuously introduced into the ESI source chamber for analysis with a syringe pump at a flow rate of 5 μL/min.

High-resolution ESI-MS/MS (HR-ESI-MS/MS) was performed on a LTQ Orbitrap XL mass spectrometer (Thermo Fisher Scientific, USA) to verify the low-resolution CID MS/MS results. Mass accuracy was calibrated before measurements according to the manufacturer's instructions to ensure operation within the <3 ppm instrument specifications. The instrument was operated in positive ion mode with the experimental parameters as follows: sheath gas flow rate, 30 arb; auxiliary gas flow rate, 8 arb; capillary voltage, 30 V; capillary temperature, 200 °C; spray voltage, 4.5 kV. The normalized CID collision energy was set to 25% (for **M1**) and 40% (for **M2**) to perform CID MS/MS experiments and the mass range was set to *m/z* 50–2000 with an isolation width of 2.0 Da. The resolution was set to 60 000 for the full scan events and 15 000 for the MS^2 scan events. A stable sample flow of 5 μL/min was introduced into the mass spectrometer by syringe pump. The automatic gain control (AGC) was activated on both instruments and the value was set to 5×10^6 and 4×10^4 for the Finnigan LCQ^{DECA} and the LTQ Orbitrap XL, respectively. All data acquired were preceded with the Qual Browser module of Xcalibur 2.1 (Thermo Fisher Scientific, Inc.).

Calculations

Standard quantum chemical calculations were carried out using density functional theory (DFT) with the aid of the Gaussian 03 suit of programs. Geometrical parameters of the structures were optimized using the B3LYP hybrid functional method with the 6-31 G*(d)* basis set. No symmetry constrains were imposed in the optimization. All optimized structures (equilibrium or transition structures) were subjected to vibrational frequency analysis for zero-point energy (ZPE) correction. The reaction pathways were traced forward and backward by the intrinsic reaction coordinate (IRC) method.

RESULTS AND DISCUSSION

Fragmentation of the two ingenol regioisomers

Each compound was injected for analysis by positive ESI-MS via a syringe pump and then fragmented in the ion trap up, and the characterization of the two isomers was realized; the spectra can be found in Fig. 2. In the discussion below, for simplicity all MS data refer to the nominal mass, and the accurate masses of the $[M+Na]^+$ ions and the crucial fragment ions are listed in Table 1.

The MS spectrum of **M1** displays an intense sodium adduct ion $[M+Na]^+$ at *m/z* 581. In MS^2 spectra, the characteristic product ion at *m/z* 353 was found as the base peak, which was proposed to be generated by loss of 228 Da from the precursor ion at *m/z* 581. The mechanism of the loss of 228 Da from the precursor ion at *m/z* 581 to give the *m/z* 353 ion may be at first sight more difficult to explain. However, it could be explained that the neighboring hydrogen migrated via a cyclic transition state for the loss of tetradecanoic acid. For

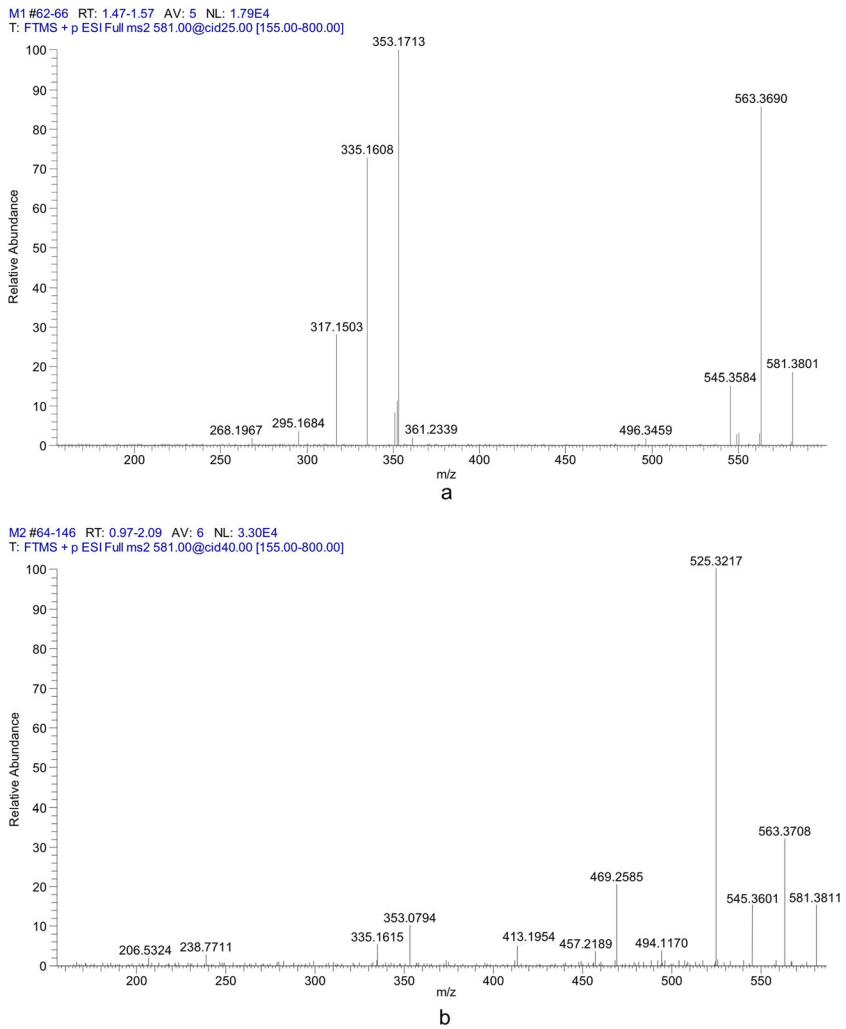

Figure 2. The ESI-HR-MS/MS spectra of (a) **M1** and (b) **M2**. Fragmentation energy was 25% (for **M1**) and 40% (for **M2**). Label threshold was set to 3%.

Table 1. Accurate mass data of molecular ions and main product ions by HR-ESI-MS/MS analysis for **M1** and **M2**

Compounds	Measured mass	Calculated mass	Elemental composition	Error (ppm)	Relative abundance (%)
3-*O*-tetradecanoylingenol (**M1**)	581.3801	581.3818	$C_{34}H_{54}O_6Na^+$	–2.92	18.5
	563.3690	563.3712	$C_{34}H_{52}O_5Na^+$	–3.73	85.4
	545.3585	545.3607	$C_{34}H_{50}O_4Na^+$	–4.03	15.2
	353.1713	353.1729	$C_{20}H_{26}O_4Na^+$	–4.53	100
	335.1608	335.1623	$C_{20}H_{24}O_3Na^+$	–4.48	72.0
	317.1503	317.1517	$C_{20}H_{22}O_2Na^+$	–4.41	28.4
20-*O*-tetradecanoylingenol (**M2**)	581.3811	581.3818	$C_{34}H_{54}O_6Na^+$	–1.20	15.6
	563.3708	563.3712	$C_{34}H_{52}O_5Na^+$	–0.71	30.9
	545.3601	545.3607	$C_{34}H_{50}O_4Na^+$	–1.10	8.0
	525.3217	525.3192	$C_{30}H_{46}O_6Na^+$	4.76	100
	469.2585	469.2566	$C_{26}H_{38}O_6Na^+$	4.045	20.3
	413.1954	413.1940	$C_{22}H_{30}O_6Na^+$	3.39	5.1
	353.1720	353.1729	$C_{20}H_{26}O_4Na^+$	–0.936	10.4
	335.1615	335.1623	$C_{20}H_{24}O_3Na^+$	–0.793	6.3

Rapid Communications in Mass Spectrometry

confirmation of the fragmentation patterns, accurate mass measurements were performed on an LTQ Orbitrap XL MS instrument. The measured mass (*m/z*) for the sodium adduct **M1** is *m/z* 581.3801, which has a deviation of –2.92 ppm from the calculated molecular monoisotopic mass (Table 1). For structure confirmation, fragmentation of **M1** is obtained by the application of increased fragmentor energy up to 25%. The observed ion at *m/z* 353.1713, corresponding to $[C_{20}H_{26}O_4Na]^+$, corroborated the neutral loss of $C_{14}H_{28}O_2$ (tetradecanoic acid) from the precursor ion at *m/z* 581.3801.

The precursor ion ($[M+Na]^+$) of **M2** at *m/z* 581 generated product ions at *m/z* 563, 545, 525, 469 and 413 by loss of water (18 Da), $2 \times H_2O$ (36 Da), C_4H_8 (56 Da), $2 \times C_4H_8$ (112 Da), and $3 \times C_4H_8$ (168 Da), respectively, in the MS^2 spectrum. These product ions were observed in MS/MS of **M2** under the collision energy of 40% or higher; lower collision energy only produces ions generated from water loss. Despite the commonly seen water loss fragmentation, **M2** showed quite a different fragmentation pathway on the tetradecanoyl chain by comparison with **M1**. For **M1**, elimination of tetradecanoic acid from the precursor ion results in an ion at *m/z* 353. However, for **M2**, sequential losses of three molecules of butylene were observed. The results have also been confirmed by HR-ESI-MS/MS (Table 1): *m/z* 525.3217 corresponded to $[C_{30}H_{46}O_6Na]^+$, *m/z* 469.2585 corresponded to $[C_{26}H_{38}O_6Na]^+$ and 413.1954 corresponded to $[C_{22}H_{30}O_6Na]^+$, respectively. The key fragmentation pathways of **M1** and **M2** (tetradecanoic acid loss for **M1** and sequential losses of butylene for **M2**) are also shown in Fig. 1.

Investigation of the fragmentation mechanism

In order to gain qualitative insights into the relative energies of the key fragmentation pathways of **M1** and **M2**, we have carried out a series of DFT calculations using the Gaussian 03 program suit at the B3LYP level of theory with the 6-31 G*(d)* basis set. All the calculations were performed on the simplified

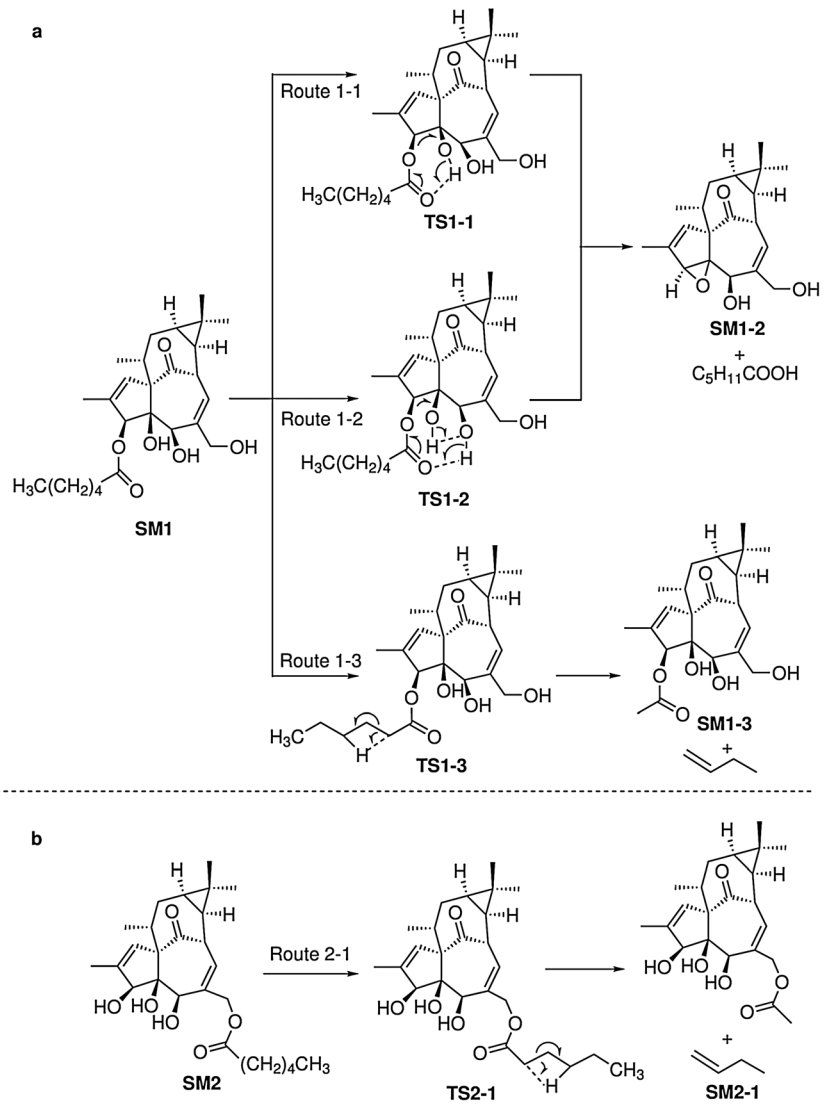

Scheme 1. Proposed mechanisms of the key fragmentation routes of the simplified models of (a) **M1** and (b) **M2**.

models of **M1** and **M2** (hexanoyl group instead of tetradecanoyl group, labeled as **SM1** and **SM2**, respectively) to reduce the computational load. According to the geometries of the optimized structures, the mechanisms of the key fragmentation and some possible routes of **SM1** and **SM2** were proposed and are shown in Scheme 1 (geometric coordinates of the structures involved in the calculations can be found in the Supporting Information). For **SM1**, the formation of **SM1-1** corresponded to neutral losses of a hexanoic acid, which may be triggered by the proton migration from the neighboring hydroxyl group to the carbonyl oxygen of hexanoyl through two possible routes (**Routes 1-1** and **1-2**). Unlike **SM1**, proton transfer was not able to happen in **SM2** due to spatial obstacles. The energy requirement of the butylene loss from **SM1** and **SM2** was calculated to explain the sequential losses of three molecules of butylene observed in the MS/MS experiments performed on **M2**.

Theoretical computations were invoked to quantitatively describe the energy requirements of the routes of the proposed mechanisms in Scheme 1 and to show the possible existence of some transition states and intermediates involved in the fragmentation pathways. By calculation, the energies and the geometries of the reactants, products and the corresponding transition states involved in the proposed mechanisms were acquired, and a schematic potential energy surface of the reactions is given in Fig. 3.

For **SM1**, the proton transfers from C4-OH to the carbonyl group of its hexanoyl group by **Route 1-1** through a six-membered-ring transition state 1-1 (**TS1-1**), leading to the breakage of the C3–O bond resulting in the formation of **SM1-1** corresponding to the neutral loss of hexanoic acid. Alternatively, the formation of the product ion and neutral loss as mentioned in **Route 1-1**, may also result from **Route 1-2**, in which the proton of the hydroxyl group on C5 transferred to the carbonyl oxygen of the hexanoyl chain, and the proton of the hydroxyl group on C4 migrated to its neighboring oxygen of C5-OH at the same time, through a transition state 1-2 (**TS1-2**). The activation barriers of **TS1-1** and **TS1-2** were calculated to be 44.5 kcal/mol and 29.7 kcal/mol (energy of **SM1** as 0 kcal/mol), respectively. The calculation results showed that **TS1-2** was more favorable than **TS1-1** by 14.8 kcal/mol in terms of the activation energy. On the other hand, the energy barrier of the loss of butylene from **SM1** (**TS1-3**) through **Route 1-3** was 94.2 kcal/mol which was far higher than those of **TS1-1** and **TS1-2**. The results mentioned above imply that loss of tetradecanoic acid through a **Route 1-2**-like pathway was more accessible than the loss of butylene for **M1** in terms of energy.

For **SM2**, theoretical calculations of energy barriers of the transition state of butylene loss from **SM2** (**TS2-1**, though **Route 2-1**) was performed, and found the energy barrier of **TS2-1** was 89.3 kcal/mol (energy of **SM2** as 0 kcal/mol). Although the activation barrier of **TS2-1** is relatively high, loss of butylene from **M2** via a **Route 2-1**-like pathway was possible when it was fragmented under high collision energy (e.g. 40%). In summary, for **SM2**, after activation by a relatively high activation energy of about 89.3 kcal/mol, butylene loss from the hexanoyl chain was triggered; the likely process also happened to **M2**, and explains the phenomenon observed in MS/MS experiments.

With the aid of calculation results, the key fragmentation mechanisms of **M1** and **M2** were confirmed and the main fragmentation pathways are proposed in Scheme 2 to describe the major product ions observed in tandem mass spectrometry experiments.

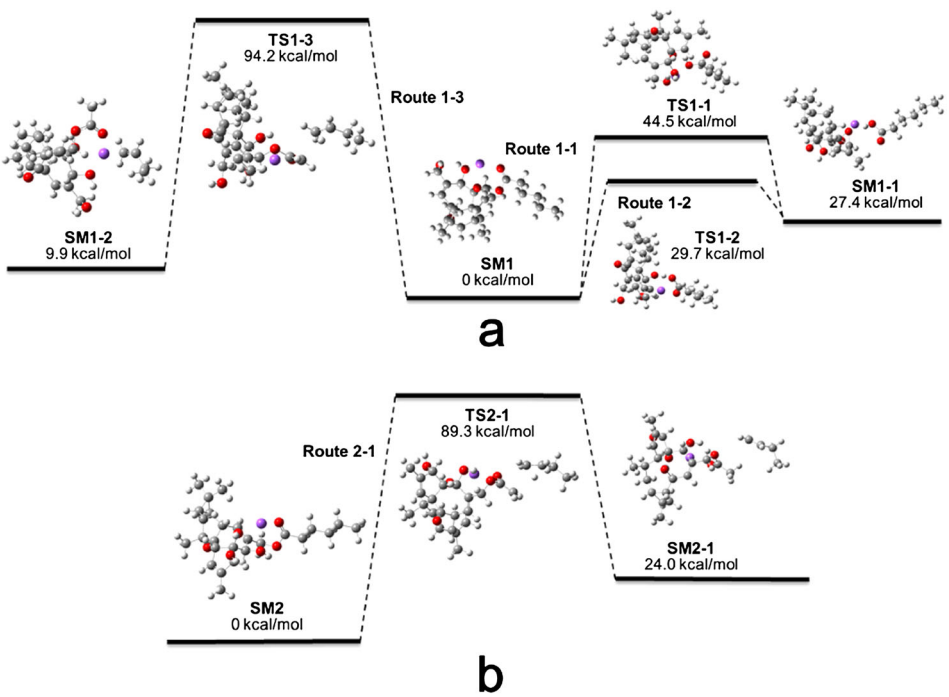

Figure 3. Potential energy profiles of the simplified models of (a) **M1** and (b) **M2**.

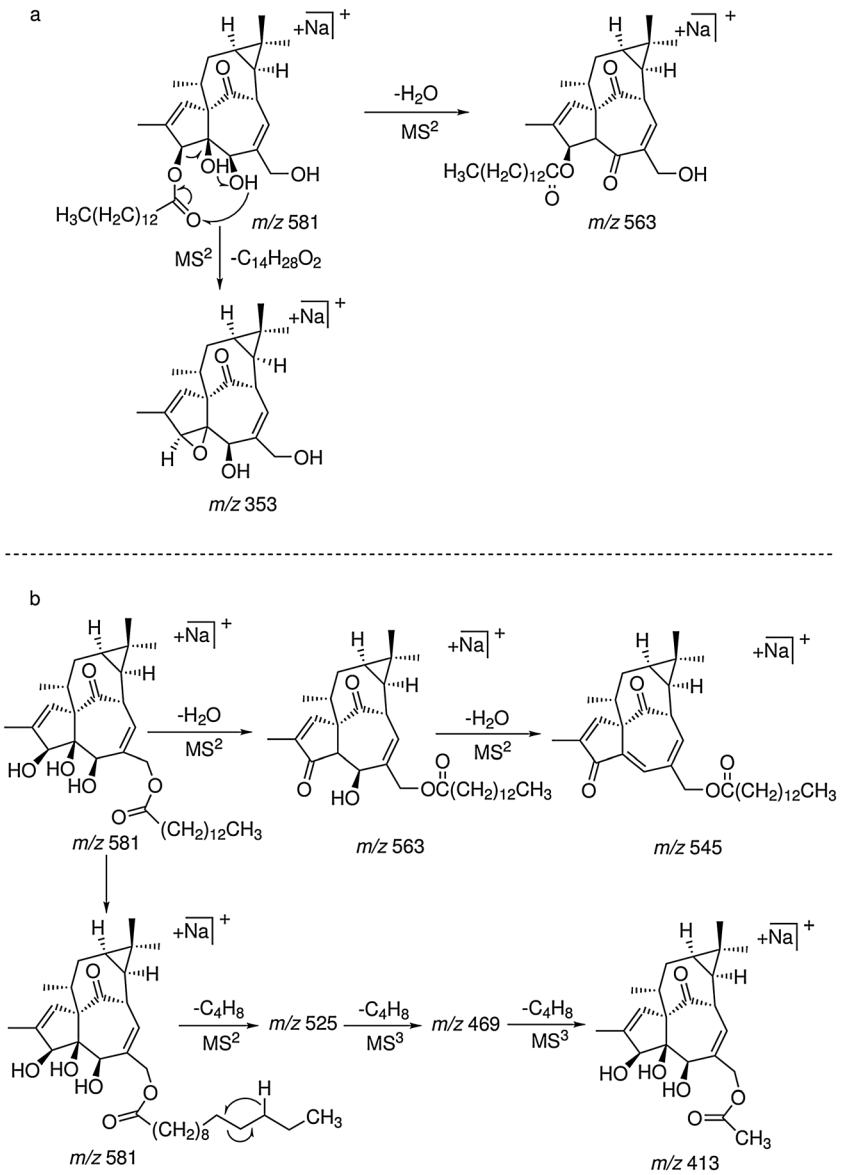

Scheme 2. Proposed fragmentation pathways to explain the formations of the main product ions from precursor ions (a) **M1** and (b) **M2**.

CONCLUSIONS

The dissociation pathways of two regioisomers (3-*O*-tetradecanoylingenol (**M1**) and 20-*O*-tetradecanoylingenol (**M2**)) from *Euphorbia wallichii* were investigated by ESI-MS/MS, from which two diagnostic fragment patterns were acquired. According to the MS/MS results, the fragmentation mechanisms of these two compounds were proposed and verified by calculating the energies of the reactants, products and the corresponding transition states using DFT calculations. These results were very valuable for the analysis and rapid identification of the derivatives of ingenol in the natural products field. Furthermore, using of DFT calculations to shed light on these reaction mechanisms showed notable prospect of application in mass spectrometry studies of natural products.

SUPPORTING INFORMATION

Additional supporting information may be found in the online version of this article.

Acknowledgements

This work was supported by grants from the National Natural Sciences Foundation of China (Nos. 30973634; 21072185), 2010 Technological Talents Program of the Chinese Academy of Sciences, granted to Dr. Y. Zhou, and a Syngenta PhD fellowship awarded to B. Xia.

REFERENCES

[1] Z. Cai, F. S. C. Lee, X. R. Wang, W. J. Yu. A capsule review of recent studies on the application of mass spectrometry in the analysis of Chinese medicinal herbs. *J. Mass Spectrom.* **2002**, *37*, 1013.
[2] W. A. Korfmacher, K. A. Cox, M. S. Bryant, J. Veals, K. Ng, C. C. Lin, R. Watkins. HPLC-API/MS/MS: a powerful tool for integrating drug metabolism into the drug discovery process. *Drug Discov. Today* **1997**, *2*, 532.
[3] X. K. Ouyang, M. C. Jin, C. H. He. Simultaneous determination of four sesquiterpene alkaloids in *Tripterygium wilfordii* Hook. F. extracts by high-performance liquid chromatography. *Phytochem. Anal.* **2007**, *18*, 320.
[4] R. B. van Breemen, C. R. Huang, Z. Z. Lu, A. Rimando, H. H. S. Fong, J. F. Fitzloff. Electrospray liquid chromatography/mass spectrometry of ginsenosides. *Anal. Chem.* **1995**, *67*, 3985.
[5] C. Guo, J. Wan, N. Hu, K. Jiang, Y. Pan. An experimental and computational investigation on the fragmentation behavior of enaminones in electrospray ionization mass spectrometry. *J. Mass Spectrom.* **2010**, *45*, 1291.
[6] N. Hu, Y. P. Tu, Y. Liu, K. Jiang, Y. Pan. Dissociative protonation and proton transfers: fragmentation of alpha, beta-unsaturated aromatic ketones in mass spectrometry. *J. Org. Chem.* **2008**, *73*, 3369.
[7] P. Liu, N. Hu, Y. Pan, Y. Tu. Ion-neutral complexes resulting from dissociative protonation: fragmentation of alpha-furanylmethyl benzyl ethers and 4-*N*,*N*-dimethylbenzyl benzyl ethers. *J. Am. Soc. Mass. Spectrom.* **2010**, *21*, 626.
[8] Y. P. Tu. Dissociative protonation sites: reactive centers in protonated molecules leading to fragmentation in mass spectrometry. *J. Org. Chem.* **2006**, *71*, 5482.
[9] xQ. W. Shi, X. H. Su, H. Kiyota. Chemical and pharmacological research of the plants in genus Euphorbia. *Chem. Rev.* **2008**, *108*, 4295.
[10] L. Pan, P. Zhou, X. Zhang, S. Peng, L. Ding, S. X. Qiu. Skeleton-rearranged pentacyclic diterpenoids possessing a cyclobutane ring from *Euphorbia wallichii*. *Org. Lett.* **2006**, *8*, 2775.
[11] H. Wang, X. F. Zhang, X. H. Cai, Y. B. Ma, X. D. Luo. Three new diterpenoids from *Euphorbia wallichii*. *Chin. J. Chem.* **2010**, *22*, 199.
[12] S. Kupchan, I. Uchida, A. Branfman, R. Dailey, B. Fei. Antileukemic principles isolated from euphorbiaceae plants. *Science* **1976**, *191*, 571.
[13] G. Zhang, M. G. Kazanietz, P. M. Blumberg, J. H. Hurley. Crystal structure of the cys2 activator-binding domain of protein kinase C delta in complex with phorbol ester. *Cell* **1995**, *81*, 917.
[14] M. Fujiwara, K. Ijichi, K. Tokuhisa, K. Katsuura, S. Shigeta, K. Konno, G. Y. Wang, D. Uemura, T. Yokota, M. Baba. Mechanism of selective inhibition of human immunodeficiency virus by ingenol triacetate. *Antimicrob. Agents Chemother.* **1996**, *40*, 271.
[15] C. L. Zani, A. Marston, M. Hamburger, K. Hostettmann. Molluscicidal milliamines from *Euphorbia milii* var. *hislopii*. *Phytochemistry* **1993**, *34*, 89.
[16] G. Fürstenberger, E. Hecker. On the active principles of the spurge family (Euphorbiaceae). XI. [1] The skin irritant and tumor promoting diterpene esters of *Euphorbia tirucalli* L. originating from South Africa. *Z. Naturforsch. C.* **1985**, *40*, 631.
[17] D. Kamimura, K. Yamada, Preparation of 13-hydroxyingenols as VCAM-1 formation inhibitors. Jpn. Kokai Tokyo Koho JP 07,258,168, **1995**, pp. 87430r–87430r.
[18] F. J. Evans, S. E. Taylor. Pro-inflammatory, tumour-promoting and anti-tumour diterpenes of the plant families Euphorbiaceae and Thymelaeaceae. *Prog. Chem. Org. Nat. Prod.* **1983**, *44*, 1.
[19] E. H. Seip, E. Hecker. Skin irritant ingenol esters from *Euphorbia esula*. *Planta Med.* **1982**, *46*, 215.
[20] C. M. Hasler, G. Acs, P. M. Blumberg. Specific binding to protein kinase C by ingenol and its induction of biological responses. *Cancer Res.* **1992**, *52*, 202.
[21] B. Sorg, R. Schmidt, E. Hecker. Structure/activity relationships of polyfunctional diterpenes of the ingenane type. I. Tumor-promoting activity of homologous, aliphatic 3-esters of ingenol and of $\Delta^{7,8}$-isoingenol-3-tetradecanoate. *Carcinogenesis* **1987**, *8*, 1.
[22] Z. Q. Lu, M. Yang, J. Q. Zhang, G. T. Chen, H. L. Huang, S. H. Guan, C. Ma, X. Liu, D. A. Guo. Ingenane diterpenoids from *Euphorbia esula*. *Phytochemistry* **2008**, *69*, 812.

